

Communication

## Using Lidar-Derived Vegetation Profiles to Predict Time since Fire in an Oak Scrub Landscape in East-Central Florida

James J. Angelo <sup>1,\*</sup>, Brean W. Duncan <sup>2</sup> and John F. Weishampel <sup>1</sup>

<sup>1</sup> Department of Biology, University of Central Florida, 4000 Central Florida Blvd., Orlando, FL, 32816-2368, USA; E-Mail: jweisham@mail.ucf.edu

<sup>2</sup> Innovative Health Applications, Mail Code: IHA-300, Kennedy Space Center, FL, 32899, USA; E-Mail: brean.w.duncan@nasa.gov

\* Author to whom correspondence should be addressed; E-Mail: james.angelo@knights.ucf.edu; Tel.: +1-407-823-6634; Fax: +1-407-823-5769.

Received: 7 January 2010; in revised form: 2 February 2010 / Accepted: 3 February 2010 /

Published: 11 February 2010

---

**Abstract:** Disturbance plays a fundamental role in determining the vertical structure of vegetation in many terrestrial ecosystems, and knowledge of disturbance histories is vital for developing effective management and restoration plans. In this study, we investigated the potential of using vertical vegetation profiles derived from discrete-return lidar to predict time since fire (TSF) in a landscape of oak scrub in east-central Florida. We predicted that fire influences vegetation structure at the mesoscale (*i.e.*, spatial scales of tens of meters to kilometers). To evaluate this prediction, we binned lidar returns into 1m vertical by  $5 \times 5$  m horizontal cells and averaged the resulting profiles over a range of horizontal window sizes (0 to 500 m on a side). We then performed a series of resampling tests to compare the performance of support vector machine (SVM), *k*-nearest neighbor (*k*-NN), logistic regression, and linear discriminant analysis (LDA) classifiers and to estimate the amount of training data necessary to achieve satisfactory performance. Our results indicate that: (1) the SVMs perform significantly better than the other classifiers, (2) SVM classifiers may require relatively small training data sets, and (3) the highest classification accuracies occur with averaging over windows representing sizes in the mesoscale range.

**Keywords:** lidar; classification algorithms; support vector machines; oak scrub; Florida; time since fire; prescribed burning; disturbance ecology

---

## 1. Introduction

Forest ecologists and managers have long recognized that disturbance plays a major role in determining the physical structure of vegetation [1,2]. Vegetation structure is three-dimensional, with both horizontal and vertical components [3]. Vertical structure, which is defined as the top-to-bottom spatial arrangement of vegetation above the ground, is affected by disturbance primarily through the mechanism of forest succession [2,3]. For example, vegetation patches that have experienced more recent disturbance will differ in their vertical structure than patches in later successional stages [4].

Fire is both a naturally and anthropogenically produced disturbance that influences the horizontal and vertical structure of vegetation across a diverse array of ecosystems, from grasslands to shrublands to forests [5,6]. Human activity—either directly through fire suppression or indirectly through clearing and/or fragmentation of vegetation—has dramatically altered natural wildfire regimes throughout the continental United States [7]. Knowledge of land-use legacies, including the history of fire and other key disturbance processes, has therefore become increasingly important for the effective conservation and management of forest ecosystems [8,9].

A crucial component of such knowledge is basic information about disturbance history, such as the time since the last disturbance and the frequency of disturbance. For fire disturbance, such information was traditionally obtained via fire scar analysis, either through field sampling of tree rings [10] or a combination of field observations and remotely sensed imagery [11]. Field sampling is resource-intensive and is typically limited to small scales, such as a few forest stands. While imagery attained via passive remote sensing facilitates analysis at broader scales, it can only delineate two-dimensional surface patterns and the optical fire scar “signal” becomes increasingly obscure as vegetation regrows [12]; consequently, the effectiveness of passive imagery may be limited in ecosystems characterized by rapid post-fire regeneration of vegetation, such as Florida scrub [13].

Airborne light detection and ranging (lidar) is an active remote sensing technology that is capable of capturing the three-dimensional structure of vegetation at high resolutions (both vertical and horizontal) and over relatively broad spatial extents [14]. While numerous researchers have reported on the ability of lidar data to characterize the vertical structure of vegetation (see [15] for a recent review), most ecologically-oriented studies incorporating lidar have relied on relatively simple lidar-derived metrics, such as canopy height [16,17]. As Hurtt *et al.* [17] noted, however, there is potentially an enormous wealth of information about the state of terrestrial ecosystems contained in the vertical profiles of vegetation derived from lidar data. Næsset [18] introduced a technique for generating vertical profiles from discrete-return lidar data by counting the density of laser returns occurring in bins of equal height in the column that extends vertically over an area with a fixed horizontal cell size. More recently, researchers have employed vertical profiles derived from discrete-return lidar data in a growing number of applied ecological studies, including studies of the effects of invasive plants on avian communities [19], the classification of land cover in the wildland-urban interface [20], and the prediction of successional states in a multistory forest [21].

In this study, we used vertical profiles derived from discrete-return lidar data in conjunction with advanced classification techniques to predict the time since fire (TSF) status of the vegetation in an oak scrub ecosystem on the east-central coast of Florida. We expected that—all other things being equal—patches of vegetation with different TSF values should exhibit distinct structural patterns, and

that these structural differences would be captured by the binned lidar returns of the vertical profiles. Thus, we predicted that the lidar-derived vertical profiles could be used to classify the TSF of the vegetation. We used nonparametric classification algorithms known as support vector machines (SVMs) to test the accuracy of this prediction, and then we conducted resampling tests to compare the performance of the SVMs to other common classification techniques and to estimate the amount of training data necessary to achieve optimal classification results.

## 2. Methods

### 2.1. Study Area

The study area is located in east-central Florida on the Atlantic coast of the United States (28.47°N and -80.67°E), and consists of approximately 200 ha of federally-owned land near the southern boundary of the Kennedy Space Center/Merritt Island National Wildlife Refuge (KSC/MINWR). The elevation in the area ranges from 1 to 3.5 m above sea level due to a ridge-swale topography formed from relict beach dunes of the Pleistocene [22]. Upland sites (also known as scrub ridges) are characterized by well-drained soils and evergreen shrub oaks, primarily sand live oak (*Quercus geminata*), Chapman's oak (*Q. chapmanii*), and myrtle oak (*Q. myrtifolia*). Mesic flatwoods are dominated by shrubs in the understory, including saw palmetto (*Serenoa repens*) and lyonia (*Lyonia* spp.), with interspersed swale marshes (*Spartina bakeri*) and sparse clusters of open-canopy slash pine (*Pinus elliotii*). This combination of scrub communities and pine flatwoods is sometimes called "scrubby flatwoods," but shall be referred to exclusively as "oak scrub" for the remainder of this manuscript (*sensu* [22]).

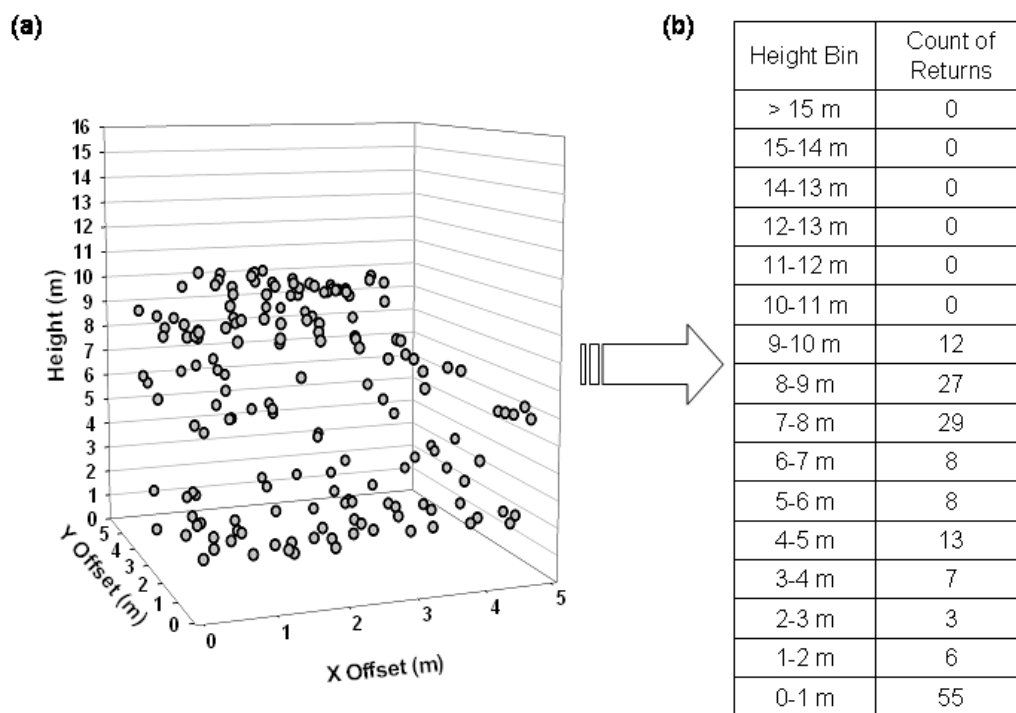
Oak scrub is a fire-maintained system that burns every 5–20 years under natural conditions [23]. Oak scrub vegetation recovers rapidly after fire and thus requires frequent burning to maintain its characteristic structure of numerous sandy openings, a sparse herb layer, little or no tree cover, and relatively dense shrub cover at heights of 1 to 2 m [23,24]. In the prolonged absence of burning, oak scrub vegetation becomes fire-resistant and undergoes structural changes toward xeric hammock [23]. Wildfire was suppressed throughout much of the KSC/MINWR area from the 1950s until 1981, when the National Aeronautics and Space Administration (NASA) instituted a prescribed burning program to reduce the buildup of vegetative fuel loads in the area [25].

### 2.2. Lidar Data Acquisition and Pre-Processing

The lidar data were acquired by the National Center for Airborne Laser Mapping (NCALM) in June of 2008 with an Optech GEMINI Airborne Laser Terrain Mapper (ALTM) mounted on a Cessna Skymaster airplane. The ALTM operated at a wavelength of 1,047 nm with a pulse repetition rate of 70 kHz, yielding a laser return density of approximately 4.2 points m<sup>-2</sup> and an average positional error of <0.4 m in both the horizontal and vertical directions (M. Sartori, personal communication). NCALM delivered the lidar point cloud data in industry-standard .LAS format, with individual returns classified as ground, non-ground, or low noise. From the point cloud data, we produced a high-resolution (1 m) bare earth digital elevation model (DEM) using FUSION lidar-processing software [26] to apply median smoothing filters and spike removal algorithms to the ground points.

We then input the bare earth DEM and the non-ground lidar points into FUSION to generate vertical height bins for the vegetation returns; since the study area contained very few human-made structures, we assumed that all non-ground laser returns were reflected from vegetation. For each  $5 \times 5$  m horizontal cell, we created vertical bins containing the number of laser returns recorded in every 1 m height interval from 0 to 15 m above the ground, with the final bin containing all returns above 15 m (Figure 1). We used a  $5 \times 5$  m cell size to match the resolution of the managed fire dataset (see next paragraph and [25]), which contained burn units as thin as 5 m on a side.

**Figure 1.** Creation of vertical height bins from the lidar point cloud data. (a) Three-dimensional profile of a  $5 \times 5$  m cell within the study area, with grey circles representing vegetation points whose heights have been normalized using the bare-earth surface raster. (b) Multidimensional output data, showing the number of vegetation point returns occurring in each of the 1 m vertical height bins.



In addition to the vertical height bins, we associated a land use/land cover (LULC) code to each  $5 \times 5$  m horizontal cell to control for *a priori* differences in vegetation structure. We assumed that, on average, cells belonging to different LULC classes would possess fundamentally different vegetation structure, as reflected by the vertical distributions of their lidar returns. To accurately predict time since fire, therefore, it was necessary to include the LULC codes as one of the input values to the classifications. The LULC code for each cell was identified as the centroid value obtained from the 2004 St. Johns River Water Management District (SJRWMD) Land Cover/Land Use dataset [27]. The predominant LULC class was *Herbaceous upland non-forested*, which comprised almost 63% of the study area, followed by *Mixed wetland hardwoods* (17%), *Non-forested wetlands* (13%), *Mixed upland non-forested* (5%), and *Surface water collection ponds* (2%). The time since fire (TSF) value for each cell was assigned in a similar manner using the managed fire dataset from KSC/MINWR [25].

### 2.3. Data Analyses

To predict the TSF value of each of the cells within the study area, we used the support vector machine (SVM) implementation provided in the *kernelab* package [28] of the R statistical software program [29]. SVMs are distribution-free machine learning algorithms that typically employ nonlinear kernel functions to perform classification and regression on high-dimensional datasets [30], often achieving significantly better results than comparable parametric techniques (e.g., see [31]). We chose the Gaussian radial basis function (RBF) kernel for our SVM classifiers, since RBF kernels have yielded extremely high accuracy rates for the most challenging high-dimensional remote sensing classifications, such as those involving hyperspectral imagery or a combination of hyperspectral imagery and lidar data [31,32].

Because we expected the distinct vertical patterns in vegetation structure associated with the different TSF values to occur at the mesoscale (*i.e.*, across horizontal extents of tens of meters to kilometers), we wrote a moving window algorithm to calculate the mean number of lidar returns in each vertical height bin occurring within a fixed-sized window from the center of each  $5 \times 5$  m cell in the study area, and then varied the window size (in  $m \times m$ ) between 0 and 500 in increments of 20. A larger window size meant that the lidar returns were averaged over a wider spatial area, but the horizontal resolution of the classified (*i.e.*, the output) raster was maintained at  $5 \times 5$  m. We simultaneously increased the SVM cost constraint parameter,  $C$ , from 1 to 8,192 by powers of two (*i.e.*, from 20 to 213). The constant  $C$ , also known as the “regularization parameter,” penalizes the SVM for misclassification errors; thus, higher values of  $C$  can improve the classifier accuracy but leads to longer computation times [31]. We used a fivefold cross-validation procedure to estimate the error rate of each combination of moving window size and  $C$  parameter. Fivefold cross-validation is a widely-used technique for estimating the error rate of a classifier when it is applied to a novel test set of data, and the resulting estimate is known as the “prediction error rate” or “generalization error” [33,34]. Thus, we selected the SVM classifier with the lowest prediction error rate.

Next, we compared the performance of the optimal SVM classifier to a set of alternative classification methods commonly applied to ecological data. Linear discriminant analysis (LDA) and logistic regression are parametric techniques that construct linear boundaries to separate data entities into classes [34]. LDA assumes that the predictor variables are normally distributed and uses least squares techniques for parameter estimation, while logistic regression assumes that predictors are binomially distributed and utilizes maximum likelihood estimation. While both of these classification techniques have been widely used, their suitability for analyzing ecological datasets has been questioned, given the nonlinear interactions that characterize most ecosystems (e.g., see [33]). Finally,  $k$ -nearest neighbor ( $k$ -NN) classifiers are nonparametric, instance-based methods that assign class membership based on a majority vote of the most similar (*i.e.*, “nearest” in Euclidean feature space) neighbors [34]. In performance tests on spatially-explicit ecological datasets,  $k$ -NN classifiers have outperformed classifiers based on linear models [33].

To compare the performance of the different classifiers and to estimate the amount of training (*i.e.*, field or “ground-truth”) data necessary to achieve satisfactory classification results, we used a bootstrap resampling methodology. For sample sizes comprising 5%, 10%, 15%, and 20% of the total study area, we generated sets of 1,000 random, stratified samples with replacement. Each sample was

stratified such that it contained all combinations of TSF and LULC codes in approximately the same proportions as they were represented in the complete data set. We then used each sample to train SVM,  $k$ -NN, LDA, and logistic regression classifiers. The LDA and proportional odds logistic regression (POLR) classifiers came from the *MASS* package built-into the R software, and these classifiers permitted no performance tuning [29]. The  $k$ -NN implementation came from the *class* package of R, and we used fivefold cross-validation to determine the optimal number of neighbors,  $k = 3$ . Finally, we tested each of the classifiers on the un-sampled portion of the data set and calculated the proportion correct and the kappa coefficient for each sample classification. The kappa coefficient, also known as the “proportion of specific agreement,” is an estimate of classification accuracy corrected for chance agreement between classes, and thus is a more conservative metric than the raw proportion correct [34]. From the bootstrap samples, we derived 95% confidence intervals for both the proportion correct and kappa coefficient attained by the four different types of classifier at each of the sample sizes.

### 3. Results

In general, increasing the value of the SVM cost parameter,  $C$ , led to a lower prediction error rate for the classifier (Figure 2). Beyond a threshold of  $C = 7,000$  (*i.e.*, a  $\log_2 C \approx 12.8$ ), however, the SVM classification algorithm was unable to converge on a solution. For a given value of  $C$ , increasing the size of the moving window resulted in an initial decline in the prediction error rate, followed by a subsequent increase in the error rate beyond a certain window size. As highlighted in Figure 2, the minimum prediction error rate of  $\approx 0.0151$ , or just over 1.5%, occurred with a moving window size of  $320 \times 320$  m and  $C = 7,000$ . The results of the classification using these optimal SVM parameters are depicted as a thematic map in Figure 3. As shown in the map, the vast majority of the misclassification errors occurred in the cells on the border between patches with different TSF values.

The results of the bootstrap resampling analyses indicate that the SVM classifier achieved significantly higher accuracy than the other classifiers tested in this study, as indicated by both the proportion correct and kappa coefficient metrics (Figure 4). The mean proportion correct and kappa coefficient values are greater for the SVM than the other classifier types for all of the sampling proportion sizes considered (5%, 10%, *etc.*); furthermore, the confidence intervals for the SVM do not overlap those of the other classifiers, indicating that these results are significant at the 95% confidence level. Finally, Figure 4 suggests that a training sample comprised of as little as 10% of the total study area may achieve classification accuracy of  $>95\%$  (in terms of proportion correct), assuming it is possible to obtain a training sample that is representative of the overall study area based on proportional class membership.

**Figure 2.** The prediction error rate (z-axis), estimated using fivefold cross-validation, as a function of varying the moving window size for averaging the lidar returns (x-axis) and the log2 of the cost parameter C (y-axis). As indicated by the red circle and the red dotted lines, the minimum prediction error rate of  $\approx 0.015$  was attained with a window size of  $320 \times 320$  m and  $C = 7,000$ . The prediction error rates for window sizes less than  $140 \times 140$  m were all higher than those for the window sizes shown on the figure and, thus, were omitted for clarity.

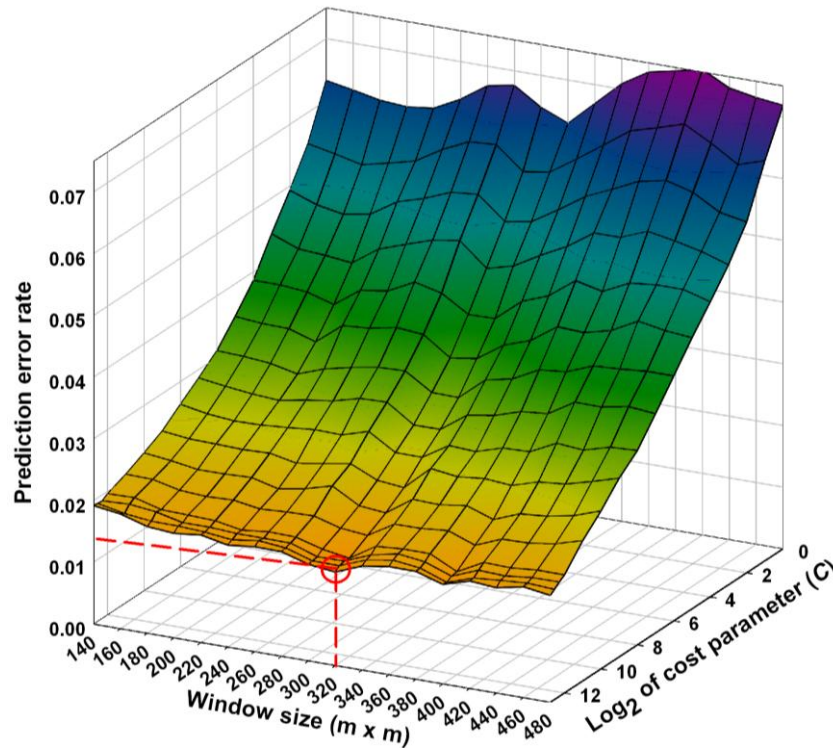


**Figure 3.** Results of SVM classification using a moving window size of  $320 \times 320$  m and a cost parameter  $C = 7,000$ . Each cell in the map is  $5 \times 5$  m in size. Green cells were classified with the correct time since fire (TSF), and the shade of green indicates the actual TSF value (see [25] for additional details on the TSF dataset). Yellow cells were misclassified, and blue cells denote reservoirs and surface water collection ponds within the study area.

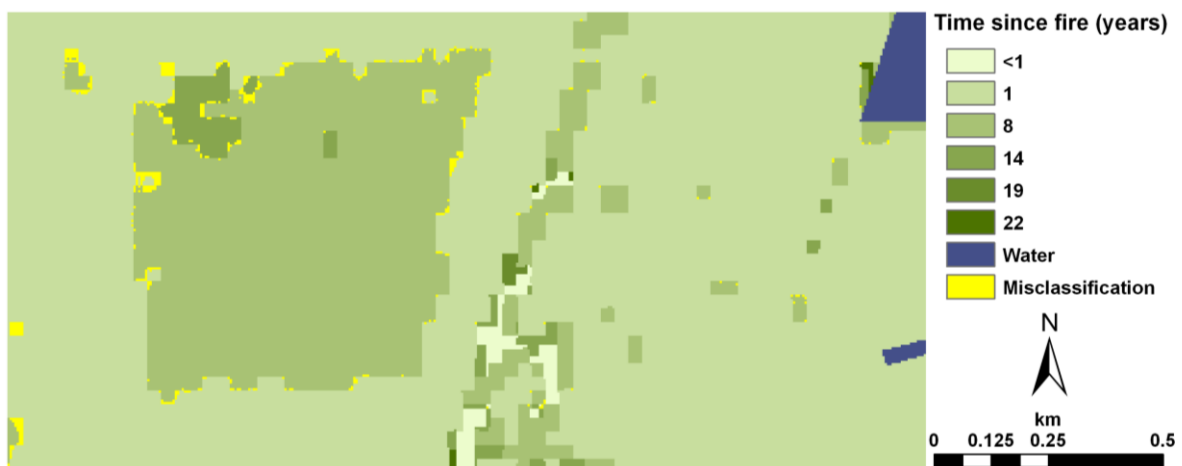
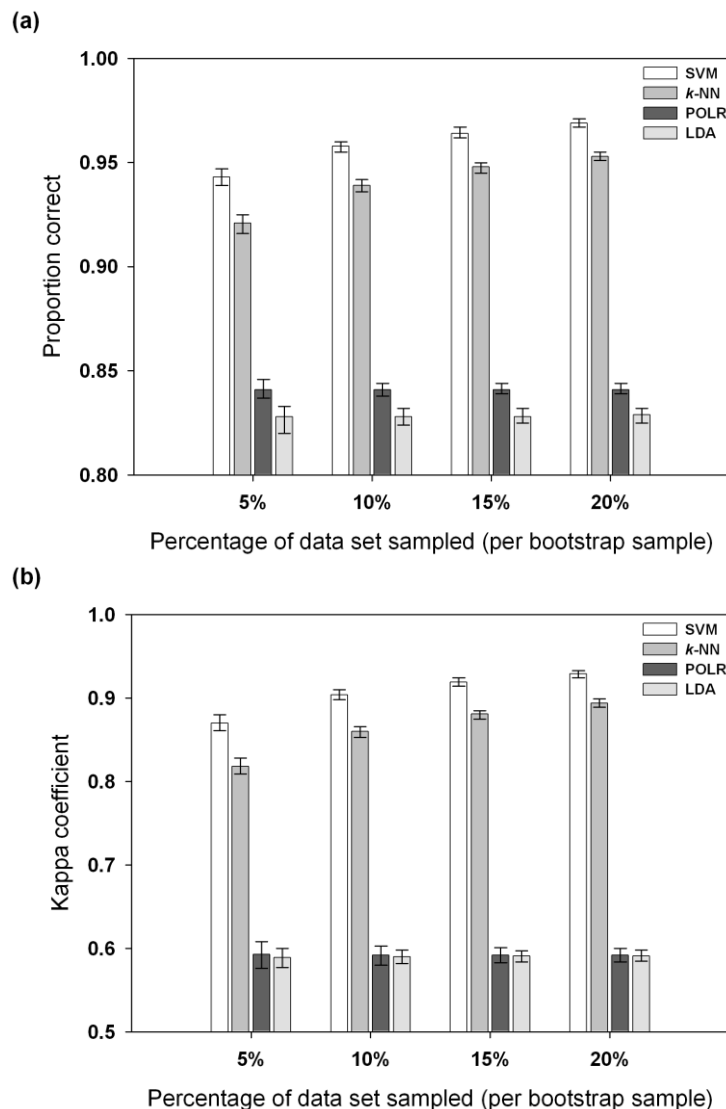


**Figure 4.** Results of the bootstrap resampling analyses. (a) Proportion correct and (b) kappa coefficient values for the support vector machine (SVM),  $k$ -nearest neighbor ( $k$ -NN), proportional odds logistic regression (POLR), and linear discriminant analysis (LDA) classifiers. Bar heights represent mean values, and error bars indicate 95% confidence intervals obtained from resampling analyses using  $n = 1,000$  bootstrap samples for each of the sample size percentages listed on the x-axis.



#### 4. Discussion and Conclusions

Our results indicate that discrete lidar returns that have been aggregated into vertical height bins can be used as input data to SVM algorithms to predict the TSF status of Florida oak scrub with extremely high levels of accuracy. Based on fivefold cross-validation, the SVM classifier with optimal parameters achieved a predicted error rate of 0.0151, or an expected accuracy of almost 98.5%. While these results were obtained by using the entire data set to train and validate the SVM classifier (*via* the cross-validation process), the results of the bootstrap analyses demonstrated that comparable levels of accuracy could be obtained using much smaller training set sizes. For example, training samples representing only 10% of the entire data set achieved proportion correct values whose 95% confidence

intervals exceeded 0.95, while the training samples comprising 20% of the data set achieved proportion correct values approaching 0.97 (Figure 4). Together, these results suggest that an SVM classifier trained using binned lidar data may generalize well to predicting TSF in novel landscapes of Florida oak scrub. To truly test the predictive power of an SVM (or any classifier, for that matter), however, one must test the classifier on one or more data sets that are independent from the data used for training and validation [34], and this points to an important area for future research.

As expected, the performance of the SVM classifier was superior to that of the classifiers based on linear models. Both LDA and logistic regression classifiers assume that predictors follow known probability assumptions and that classes can be separated with linear boundaries. As discussed earlier, however, these assumptions are unlikely to hold in many complex ecological systems. While logistic regression achieved slightly higher accuracy than LDA in terms of proportion correct, the two classifiers produced kappa coefficients with overlapping 95% confidence intervals, and thus did not differ from a statistical perspective (Figure 4). The nonparametric  $k$ -NN classifier outperformed the LDA and logistic regression classifiers, which is consistent with previous work showing that  $k$ -NN has superior predictive power over linear models on spatially-connected ecological data sets [33]. Still, the SVM outperformed the  $k$ -NN classifier in terms of both proportion correct and kappa coefficient accuracy measures. While it would be interesting to compare the performance of SVMs against other advanced machine learning classifiers (such as artificial neural networks or RandomForest decision trees), such a comparison was beyond the scope of the present study.

We achieved optimal performance with the SVM classifier by averaging the lidar returns in the vertical bins over a window of  $320 \times 320$  m from the center of each cell, a spatial scale that clearly falls within the range considered to be the “mesoscale” [35]. Thus, fire appears to be a dominant pattern-generating mechanism at the mesoscale, and this pattern is reflected in the vertical structure of the oak scrub vegetation in our study site. It should be noted, however, that Holling [35] formulated his hypothesis primarily in the context of natural disturbance regimes, while the current fire regime in our study area is based on prescribed burning. One might argue, therefore, that the success of our technique in predicting TSF is due in large part to the relative homogeneity of structure created by prescribed burning, a commonly-raised concern regarding the efficacy of anthropogenic fire management regimes (e.g., see [36]). The application of our methodology to other areas characterized by natural disturbance regimes will address this concern.

Hurt et al. [17] argued: “There is a potential wealth of information in lidar profiles and their spatial distributions” that, at the time of their writing, was “largely unexplored.” On the other hand, ecologists have long recognized that vegetation patches that have experienced more recent disturbance will differ in their vertical structure than patches in later successional stages [1,4]. The results of our study and other recent studies (e.g., [16,21]) suggest that vertical profiles derived from discrete-return lidar data can characterize these differences in the three-dimensional structure of vegetation, and that natural resource managers can then use these profiles to predict successional status with a high degree of accuracy. Furthermore, since many landscapes require a mosaic of vegetation patches in various structural stages to maintain a full complement of native species, there is an enormous potential for lidar data to serve as a management tool. It is our hope that the growing availability of lidar-derived datasets, combined with powerful techniques such as the one discussed in this paper, will provide ecologists and resource

managers with additional tools to help them meet the daunting challenge of maintaining the ecological integrity of natural systems in the face of ever-growing anthropogenic influences.

### Acknowledgements

We thank Ross Hinkle, Reed Noss, and Pedro Quintana-Ascencio for their insightful comments regarding the manuscript. We would also like to acknowledge Michael Sartori, Sidney Schofield, and Ramesh L. Shrestha at the National Center for Airborne Laser Mapping (NCALM) for acquiring the lidar data used in this project through the NCALM Seed Proposal program, Don Doerr and the NASA KSC security team for coordinating the lidar acquisition flight over the study area, and the US Fish & Wildlife Service MINWR staff for logistical support. This work was supported in part through NASA Grant Number NNX08AM11G.

### References

1. White, P.S. Pattern, process, and natural disturbance in vegetation. *Bot. Rev.* **1979**, *45*, 229-299.
2. Oliver, C.D. Forest development in North America following major disturbances. *Forest Ecol. Manage.* **1980**, *3*, 153-168.
3. Brokaw, N.; Lent, R. Vertical structure. In *Maintaining Biodiversity in Forest Ecosystems*; Hunter, M., Ed.; Cambridge University Press: Cambridge, UK, 1999; pp. 373-399.
4. Tierney, G.L.; Faber-Langendoen, D.; Mitchell, B.R.; Shriver, W.G.; Gibbs, J.P. Monitoring and evaluating the ecological integrity of forest ecosystems. *Front. Ecol. Environ.* **2009**, *7*, 308-316.
5. Ahlgren, I.F.; Ahlgren, C.E. Ecological effects of forest fires. *Bot. Rev.* **1960**, *26*, 483-533.
6. Bond, W.J.; Keeley, J.E. Fire as a global 'herbivore': the ecology and evolution of flammable ecosystems. *Trend. Ecol. Evolut.* **2005**, *20*, 387-394.
7. Parisien, M.A.; Moritz, M.A. Environmental controls on the distribution of wildfire at multiple spatial scales. *Ecol. Monogr.* **2009**, *79*, 127-154.
8. Landres, P.B.; Morgan, P.; Swanson, F.J. Overview of the use of natural variability concepts in managing ecological systems. *Ecol. Appl.* **1999**, *9*, 1179-1188.
9. Foster, D.; Swanson, F.; Aber, J.; Burke, I.; Brokaw, N.; Tilman, D.; Knapp, A. The importance of land-use legacies to ecology and conservation. *Bioscience.* **2003**, *53*, 77-88.
10. Romme, W.H. Fire and landscape diversity in subalpine forests of Yellowstone National Park. *Ecol. Monogr.* **1982**, *52*, 199-221.
11. Turner, M.G.; Hargrove, W.W.; Gardner, R.H.; Romme, W.H. Effects of fire on landscape heterogeneity in Yellowstone National Park, Wyoming. *J. Veg. Sci.* **1994**, *5*, 731-742.
12. DeFries, R. Terrestrial vegetation in the coupled human-Earth system: contributions of remote sensing. *Ann. Rev. Environ. Res.* **2008**, *33*, 369-390.
13. Shao, G.; Duncan, B.W. Effects of band combinations and GIS masking on fire-scar mapping at local scales in east-central Florida, USA. *Can. J. Remote Sens.* **2007**, *33*, 250-259.
14. Lefsky, M.A.; Cohen, W.B.; Parker, G.G.; Harding, D.J. Lidar remote sensing for ecosystem studies. *Bioscience* **2002**, *52*, 19-30.
15. Omasa, K.; Hosoi, F.; Konishi, A. 3D lidar imaging for detecting and understanding plant responses and canopy structure. *J. Exp. Bot.* **2007**, *58*, 881-898.

16. Zimble, D.A.; Evans, D.L.; Carlson, G.C.; Parker, R.C.; Grado, S.C.; Gerard, P.D. Characterizing vertical forest structure using small-footprint airborne LiDAR. *Remote Sens. Environ.* **2003**, *87*, 171-182.
17. Hurtt, G.C.; Dubayah, R.; Drake, J.; Moorcroft, P.R.; Pacala, S.W.; Blair, J.B.; Fearon, M.G. Beyond potential vegetation: combining lidar data and a height-structured model for carbon studies. *Ecol. Appl.* **2004**, *14*, 873-883.
18. Naesset, E. Practical large-scale forest stand inventory using a small-footprint airborne scanning laser. *Scand. J. Forest Res.* **2004**, *19*, 164-179.
19. Boelman, N.T.; Asner, G.P.; Hart, P.J.; Martin, R.E. Multi-trophic invasion resistance in Hawaii: Bioacoustics, field surveys, and airborne remote sensing. *Ecol. Appl.* **2007**, *17*, 2137-2144.
20. Koetz, B.; Morsdorf, F.; van der Linden, S.; Curt, T.; Allgöwer, B. Multi-source land cover classification for forest fire management based on imaging spectrometry and LiDAR data. *Forest Ecol. Manage.* **2008**, *256*, 263-271.
21. Falkowski, M.J.; Evans, J.S.; Martinuzzi, S.; Gessler, P.E.; Hudak, A.T. Characterizing forest succession with lidar data: An evaluation for the Inland Northwest, USA. *Remote Sens. Environ.* **2009**, *113*, 946-956.
22. Schmalzer, P.A.; Hinkle, C.R. *Effects of Fire on Composition, Biomass, and Nutrients in Oak Scrub Vegetation on John F. Kennedy Space Center, Florida*; National Aeronautics and Space Administration: Kennedy Space Center, FL, USA, 1987; p. 149.
23. Menges, E.S. Ecology and conservation of Florida scrub. In *Savannas, Barrens, and Rock Outcrop Plant Communities of North America*. Anderson, R.C., Fralish, J.S., Baskin, J.M., Eds.; Cambridge University Press: New York, NY, USA, 1999; pp. 7-22.
24. Duncan, B.W.; Boyle, S.; Breininger, D.R.; Schmalzer, P.A. Coupling past management practice and historic landscape change on John F. Kennedy Space Center, Florida. *Landscape Ecol.* **1999**, *14*, 291-309.
25. Duncan, B.W.; Shao, G.F.; Adrian, F.W. Delineating a managed fire regime and exploring its relationship to the natural fire regime in East Central Florida, USA: a remote sensing and GIS approach. *Forest Ecol. Manage.* **2009**, *258*, 132-145.
26. McGaughey, R.J. *FUSION/LDV: Software for LIDAR Data Analysis and Visualization*. US Department of Agriculture, Forest Service, Pacific Northwest Research Station: Seattle, WA, USA, 2009; p. 123.
27. SJRWMD. *SJRWMD Land Use and Land Cover—2004*. St. Johns River Water Management District: Palatka, FL, USA, 2006.
28. Karatzoglou, A.; Smola, A.; Hornik, K.; Zeileis, A. kernlab—An S4 package for kernel methods in R. *J. Stat. Softw.* **2004**, *11*, 1-20.
29. *R: A Language and Environment for Statistical Computing*. R Development Core Team, R Foundation for Statistical Computing: Vienna, Austria, 2008.
30. Burges, C.J.C. A tutorial on support vector machines for pattern recognition. *Data Min. Knowl. Discov.* **1998**, *2*, 121-167.
31. Dalponte, M.; Bruzzone, L.; Gianelle, D. Fusion of hyperspectral and LIDAR remote sensing data for classification of complex forest areas. *IEEE Trans. Geosci. Remote Sens.* **2008**, *46*, 1416-1427.

32. Melgani, F.; Bruzzone, L. Classification of hyperspectral remote sensing images with support vector machines. *IEEE Trans. Geosci. Remote Sens.* **2004**, *42*, 1778-1790.
33. Tan, C.O.; Özesmi, U.; Beklioglu, M.; Per, E.; Kurt, B. Predictive models in ecology: comparison of performances and assessment of applicability. *Ecol. Inform.* **2006**, *1*, 195-211.
34. Fielding, A.H. *Cluster and Classification Techniques for the Biosciences*. Cambridge University Press: Cambridge, UK, 2007; p. 246.
35. Holling, C.S. Cross-scale morphology, geometry, and dynamics of ecosystems. *Ecol. Monogr.* **1992**, *62*, 447-502.
36. Brown, R.T.; Agee, J.K.; Franklin, J.F. Forest restoration and fire: principles in the context of place. *Conserv. Biol.* **2004**, *18*, 903-912.

© 2010 by the authors; licensee Molecular Diversity Preservation International, Basel, Switzerland. This article is an open-access article distributed under the terms and conditions of the Creative Commons Attribution license (<http://creativecommons.org/licenses/by/3.0/>).